Journal of Ethnopharmacology 338 (2025) 119073

Contents lists available at ScienceDirect

Journal of Ethnopharmacology

journal homepage: www.elsevier.com/locate/jethpharm

Kerstinginone, a new flavanone derivative from *Commiphora kerstingii* Engl. (Burseraceae) with potent apoptosis-inducing activity and inhibition of AKT/mTOR signaling pathway in non-sensitive prostate cancer cells

Joël Abel Gbaweng Yaya [a,b], Stephane Zingue [c,d,*], Anne Offermann [d,e], Roméo Feunaing Toko [a], Duan Kang [d], Elisée Bapong [a], Céline Henoumont [f], Sophie Laurent [f], Verena-Wilbeth Sailer [d], Jutta Kirfef [d], Emmanuel Talla [a], Sven Perner [d]

[a] *Department of Chemistry, Faculty of Science, University of Ngaoundere, P.O. Box 454, Ngaoundere, Cameroon*
[b] *Centre for Research on Medicinal Plants and Traditional Medicine, Institute of Medical Research and Medicinal Plants Studies, P.O. Box 13033, Ngaoundere, Cameroon*
[c] *Department of Pharmacotoxicology and Pharmacokinetics, Faculty of Medicine and Biomedical Sciences, University of Yaounde 1, P.O. Box 1364, Yaounde, Cameroon*
[d] *Institute of Pathology, University Hospital Schleswig-Holstein, 23538, Luebeck, Germany*
[e] *Gerhard-Domagk Institute of Pathology, University Hospital Münster, Germany*
[f] *Department of General Organic and Biomedical Chemistry, Faculty of Medicine and Pharmacy, University of Mons, Belgium, Avenue Maistriau, 19, B-7000, Mons, Belgium*

A R T I C L E I N F O

Keywords:
Commiphora kerstingii
Kerstingilactone
Kerstinginone
Prostate cancer
Cell growth
Apoptosis

A B S T R A C T

Ethnopharmacological relevance: Commiphora kerstingii Engl is a tree which is 20–30 m in height and commonly called "ararrabi" in Hausa. It is found in the Sahelian region (Cameroon, Chad, and Nigeria) where it is utilized for the treatment of several ailments including cancer.

Aim of the study: This study was aimed at investigating the chemical constituents and cytotoxic effect of extracts and isolates from the stem barks and leaves of *C. kerstingii.*

Materials and methods: Using classical chromatography technique coupled with spectroscopic analysis and literature information, ten (10) compounds were isolated from *C. kerstingii* stem barks and leaves, out of which two [kerstingilactone (**3**) and kerstinginone (**10**)] were new. To evaluate their potential cytotoxic effect, the impact on cell viability, growth, and proliferation was assessed using MTT and CCK-8 assays. Cell death mechanisms were analyzed via flow cytometry, and Western blotting was utilized to examine the expression of specific regulatory proteins. Furthermore, anti-metastatic properties were investigated through assays on cell migration, adhesion, and chemotaxis.

Results: Among the tested compounds, **2** (Masticadienonic Acid) and **10** (kerstinginone) exhibited significant dose-dependent inhibition of PC3 and LNCaP cell growth. Compound 2 displayed optimal inhibitory effects within a concentration range of 10–40 μg/mL, while compound 10 demonstrated potent growth inhibition at concentrations of 2.5–10 μg/mL. Both compounds suppressed cell proliferation and the formation of clones. Specifically, compound 2 induced apoptosis solely in the androgen-sensitive LNCaP prostate cancer cells, whereas compound 10 induced a stronger and concentration-dependent apoptotic response in both PC3 and LNCaP cells, resulting in approximately 50–70% apoptotic cells. It also induced potent cell migration/invasion arrest at concentrations ranging from 2.5 to 5 μg/mL and increased cell adhesion to the extracellular matrix.

Abbreviations: ATCC, American Type Culture Collection; ^{13}C NMR, Carbon 13 Nuclear Magnetic Resonance; CCK-8, Cell Counting Kit-8; CC, Column Chromatography; CK-EA, *Commiphora* kerstingii stem barks Ethyl Acetate; CK-EE, *Commiph*ora kerstingii stem barks Ethanolic Extract; CKL-EA, *Commiphora* kerstingii Leave Ethyl Acetate; CKL-EE, *Commiphor*a kerstingii Leave Ethanolic Extract; ECL, Enhanced Chemiluminescence; DEPT, Distortionless Enhancement by Polarization Transfer; DMSO, DimethylSulfoxide; HMBC, Heteronuclear Multiple Bound Correlation; ELISA, Enzyme-Linked Immunosorbent Assay; EGFR, Epidermal Growth Factor Receptor; EMT, Epithelial–Mesenchymal Transition; BSA, Bovine Serum Albumin; FADD, Fas-Associated protein with Death Domain; FBS, Fetal Bovine Serum; ^{1}H NMR, Proton Nuclear Magnetic Resonance; HRP, Horseradish Peroxidase; LNCaP, Human Androgen Sensitive; IR, Infra-Red; MS, Mass Spectroscopy; MTT, Mitochondrial Tetrazolium Test; PBS, Phosphate-Buffered Saline; PC3, Human Androgen Non-sensitive; PI, Propidium Iodide; pNA, p-Nitroaniline; PTEN, Phosphatase and Tensin Homolog; TMS, Tetra Methyl Silane; TLC, Thin-Layer Chromatography; UV, Ultra-Violet.

* Corresponding author. Basic and Clinical Cancer Research Unit, Department of Pharmacotoxicology and Pharmacokinetics, Faculty of Medecine and Biomedical Sciences, University of Yaounde I, P.O. Box 1364, Yaounde, Cameroon.
E-mail address: stephane.zingue@fmsb-uy1.cm (S. Zingue).

https://doi.org/10.1016/j.jep.2024.119073
Received 6 February 2024; Received in revised form 4 November 2024; Accepted 8 November 2024
Available online 9 November 2024
0378-8741/© 2024 Elsevier B.V. All rights are reserved, including those for text and data mining, AI training, and similar technologies.

Conclusion: Kerstinginone exhibits potent cytotoxicity and apoptosis-inducing activity, making it a promising lead for discovering a new anticancer drug.

1. Introduction

Prostate cancer, the second most common cancer in men globally following lung cancer, accounted for 1,414,259 new cases and 375,304 deaths in 2020, comprising 3.8% of all male cancer-related deaths (Bray et al., 2018; Ferlay et al., 2020). Its occurrence and fatality rates worldwide are closely linked to age, with the average age of diagnosis being 66 years. Without intervention, an estimated 2,293,818 new cases are projected by 2040, with a minor increase (1.05%) in mortality (Ferlay et al., 2020). Prostate cancer often lacks symptoms in its early stages and may progress slowly, requiring minimal or no treatment (Rawla, 2019). However, common symptoms include urinary difficulties, increased urination frequency, and nocturia, which can also be indicative of prostatic hypertrophy. Advanced stages may manifest as urinary retention and back pain, with the skeletal axis being the primary site for bone metastases (Prashanth, 2019).

In Africa, based on the GLOBOCAN report 2020, the highest number of new cases which summed up to 26,392 persons was recorded in western Africa. However, highest rate of mortality of 7709 deaths was recorded in the central region of Africa, ranking it second worldwide (Globocan, 2020). According to the same report, in Cameroon, prostate cancer was the major cancer occurring in men with 2189 new cases in 2020 and 1184 deaths, accounting for more than half of the diagnosed cases (Globocan, 2020). Despite significant progress in medical care, fatalities due to prostate cancer continue to rise (Pernar et al., 2018). This is especially evident in developing nations, where governments are less prepared to tackle this challenge due to limited access to diagnostic tools and the high expenses associated with treatments (Zingue et al., 2020). It is then urgent to find alternative solutions (preventive and curative) such as bioactive secondary metabolites from medicinal plants, which could be used in chemotherapy and hormone therapy.

Commiphora kerstingii Engl. belongs to the family Burseraceae, a large family comprising about 17 genera and over 600 species of tropical shrubs and trees. The major genera include *Commiphora* (185 species), *Bursera* (80 species), *Canarium* (75 species) and *Boswellia* (24 species). *C. kerstingii* is a tree which is 20–30 m in height with a smooth bark that eventually peels off leaving brownish papery strips. Its branches are covered in dense clusters of panicles, with a brownish tomentellous appearance and noticeable leaf scars, making it a popular choice for planting (Hutchinson and Dalziel, 1966). This species is called “ararrabi” or “hana gobara” (Hausa) and “kabiwal” (Fulani). It is found in the Sahelian region of Cameroon, Chad, and Nigeria. Its habitat is savannah, but often planted as a fence in towns and villages (Keay, 1964). In Northern Nigeria, *C. kerstingii* is utilized for the treatment of fever, measles, asthma, rheumatism, venereal diseases, and cancer (Mann et al., 2003).

Regarding previous research on the phytochemistry and pharmacology of this plant, authors have demonstrated the presence of various classes of natural compounds such as saponins, tannins, and volatile oils (Toma et al., 2016). In addition, numerous phytochemical investigations have been done on gums and resins of *Commiphora* species as well as the isolation and characterization of various compounds such as monoterpenes, diterpenes, sesquiterpenes, triterpenes, steroids, flavonoids, phenolic acids, etc. (Liumir et al., 2005; Chi-Yu and Jun-Li, 2018; Maria et al., 2018; Jia-Wang et al., 2018; Jing et al., 2012; Judith et al., 2022). Sallau (2009) investigated the leaves of *C. kerstingii* and isolated two isomeric pentacyclic triterpenoids named glutinol and rhoiptelenol in addition to 11-methoxy-α-Boswellic acid. Research has proven that *C. kerstingii* exhibits activity against bacteria and fungi, including *Candida albicans, Bacillus subtilis* and *Escherichia coli* (Toma et al., 2016). The scarcity of data on its potential anticancer effects prompted us to isolate compounds from *C. kerstingii* leaves and stem bark extracts and assess their cytotoxic effect on prostate cancer cell lines.

2. Materials and methods

2.1. General procedure

The melting points of the isolated compounds were measured using an Electrothermal IA9000 Series digital melting point apparatus (Bibby Scientific, Great Britain). NMR data were acquired using AVANCE II 500 and NEO 600 (Bruker) spectrometer, employing tetramethylsilane (TMS) as the standard for ^{1}H and ^{13}C NMR; IR spectra were obtained using FT-IR Spectrum 100 of PerkinElmer spectrometer and UV spectra were obtained using UV/Vis Lambda 35 of PerkinElmer spectrometer. Mass spectrometry was conducted using QTOF-MS-LD^{+} equipment. Column chromatography (CC) was carried out using silica gel (Merck, particle size 230–400 mesh) as the adsorbent, while thin-layer chromatography (TLC) was performed on silica gel pre-coated aluminium sheets (Merck KGaA).

2.2. Plant material

2.2.1. Harvest and authentication

In July 2021, stem barks and leaves of *Commiphora kerstingii* Engl (Burseraceae) were gathered in Ngaoundere, Adamawa region of Cameroon. The plant’s authenticity was confirmed by Dr. Eric T. NGANSOP (botanist from the National Herbarium of Cameroon) through comparison to a known specimen under voucher number No. 4333 SRFCam. The name of the plant was confirmed on “World flora Online".

2.2.2. Extraction

After dried and powdered stem barks of *C. kerstingii* was obtained, 2.5 kg was extracted by simple maceration using 7 L of ethyl acetate for 72 h. The filtrate was concentrated using a Bioevopeak REV-200 B rotavapor. The extraction was repeated 3 times to yield 71 g of ethyl acetate crude extract of *C. kerstingii*. The residual powder was dried and macerated in 4 L of ethanol for 72 h, three times to yield 94 g of ethanolic crude extract.

Using the same procedure with the leaves, from 1 kg of leaves powder 54 g of ethyl acetate extract and 65 g of ethanolic extract were obtained.

2.2.3. Isolation of compounds

For the isolation, 30 g of the leaves ethyl acetate extract was subjected to column chromatography using silica gel (Merck, 230–400 mesh particle size) as the stationary phase and eluted using a gradient system solvent in increasing polarity of hexane, hexane-ethyl acetate and ethyl acetate-methanol. During the elution, the fractions obtained at the bottom of the column were gradually grouped in series on the basis of their TLC profile. In some of these series, precipitates were formed and were treated by repetitive simple filtration using suitable solvents or solvent system which did not dissolve them. This is how, of the 3 series resulting from fractions obtained with the hexane/ethyl acetate 5% elution system, compounds **1** (12 mg) and **2** (38 mg) were obtained as white powder. From one of the 5 series resulting from the fractions obtained with the hexane/ethyl acetate 50% elution solvent system, compound **3** (15 mg) was obtained as brown powder. Using the same methods, compounds **4** (43 mg) and **5** (12 mg) were obtained from series

resulting of the fractions obtained with the hexane/ethyl acetate 70% elution solvent system as white powder; and compound **6** (24 mg), white powder from 2 series resulting of the fractions obtained with ethyl acetate (100%) elution solvent.

Furthermore, 50 g of the stem bark ethyl acetate extract was subjected to column chromatography using silica gel (Merck, 230–400 mesh particle size) as the stationary phase and eluted using a gradient solvent system in increasing polarity of hexane, hexane-ethyl acetate and ethyl acetate-methanol. As for the isolation procedure of the ethyl acetate extract of leaves, during the elution, the fractions obtained at the bottom of the column were gradually grouped in series on the basis of their TLC profile. In some of these series, precipitates were formed and were treated by repetitive simple filtration using suitable solvents or solvent system which did not dissolve them. Compound **7** (21 mg) was obtained as white powder from one oily serie resulting from the fractions obtained with the hexane (100%) elution solvent; compound **8** (16 mg) from series resulting from the fractions obtained with the hexane/ethyl acetate 20% solvent system as brown powder and compounds **9** (12 mg) from 2 series resulting from the fractions obtained with hexane/ethyl acetate 70% solvent system as white powder.

Compound **10** (yellow powder, 35 mg) was obtained after subjecting 5 g of the serie resulting from fractions obtained with hexane/ethyl acetate 50 % system solvent to a column chromatography on silica gel (230–400 mesh particle size) using a hexane/ethyl acetate 60 % isocratic solvent system.

2.3. Antitumor activity investigation

2.3.1. Cell culture

Human androgen-insensitive (PC3) and -sensitive (LNCaP) cell lines were obtained from the American Type Culture Collection (ATCC) Promochem located in Wesel, Germany.

LNCaP and PC3 cells were cultured and subcultured in RPMI-1640 medium supplemented with 10% fetal bovine serum (FBS), and 1% penicillin (100 U/mL)/streptomycin (100 μg/mL). They were maintained in a humidified atmosphere containing 5% CO_2 at 37 °C and a pH of 7.4. Cell passages were performed by replacing 90% of the supernatant with fresh medium every two days. Before each experiment, the number of viable cells was determined using enzyme-linked immunosorbent assay (ELISA) Multiskan TECAN reader counter system.

2.3.2. Assessment of cell growth

Cell proliferation was evaluated using 3-(4,5-dimethylthiazol-2-yl)-2,5-diphenyltetrazolium bromide (MTT) dye reduction assay (Roche Diagnostics, Penzberg, Germany). LNCaP and PC3 cells, both treated and untreated, were seeded onto 96-well plates at a density of 100 μL containing 1×10^5 cells/ml. Crude extracts and compounds derived from *C. kerstingii* were dissolved separately in DMSO and tested at concentrations ranging from 0.5 to 60 μg/mL for compounds and 2.5–200 μg/mL for extracts. Negative control cells were exposed solely to the vehicle (0.01% DMSO) and positive control cells to docetaxel (from 0.125 to 1 μM). At intervals of 0, 24, 48, and 72 h, 10 μL of MTT solution (5 mg/mL) was added to each well and incubated at 37 °C with 5% CO_2 for 2 h. Subsequently, the cells were lysed using a buffer containing 10% SDS in 0.01 M HCl for an additional 2 h. Absorbance readings at 550 nm were obtained for each well using a microplate ELISA TECAN© SPARK reader (Crailsheim, Germany).

2.3.3. Assessment of cell proliferation

The ability of compounds to inhibit cell growth was determined by the stable and non-toxic GLPBio Cell Counting Kit-8 (CCK-8) (Hamburg, Germany). Treated versus non-treated LNCaP and PC3 cells (100 μL, 1×10^4 cells/mL) were seeded onto 96-well plates and incubated (5% CO_2, 37 °C) for 24 h. Thereafter, 10 μL of the retained compounds were tested at concentrations of 0.5–40 μg/mL, while the control was exposed to the vehicle (DMSO 0.01%). After 48 h of incubation, 10 μL of CCK8 solution was added to each well of the plate and incubated for 4 h (5% CO_2, 37 °C). Plates were gently agitated on a shaker and absorbance was read at 450 nm using a microplate TECAN reader.

2.3.4. Assessment of the inhibition of clone formation

Treated versus non-treated PC3 cells were transferred onto 6-well plates at 500 cells per well. Retained compounds (**2** and **10**) were then added at the optimal concentration. Following 7 days of incubation, colonies ≥50 cells were counted. The number of clones in the control was set to 100% and compared to the number of clones of treated tumor cells.

2.3.5. Flow cytometry for detection of apoptotic cells

To understand the mechanism of cell growth inhibition induced by the retained compounds (**2** and **10**), staining was done using Annexin V/propidium iodide (PI) purchased from BD Pharmingen (Heidelberg, Germany). The PC3 and LNCaP cells were incubated with the compounds at respective efficacy concentrations for 48 h. Thereafter, they were rinsed with PBS two times and incubated in the dark at room temperature for 15 min with 5 μL each of Annexin V-FITC and propidium iodide. Flow cytometry analysis was performed on the cells with FACS caliber from BD Biosciences (Heidelberg, Germany). The percentages of early and late apoptotic cells, as well as necrotic or viable cells, were computed.

2.3.6. Caspase-3/CPP32 colometric assay

The capability of the retained compounds (**2** and **10**) to activate caspases-3 (Cysteinyl aspartate-specific protease), the hallmark of intrinsic apoptosis activation in mammalian cells was assessed using Caspase-3/CPP32 colorimetric assay Kit (Ilmenau, Germany). This assay detects the chromophore p-nitroaniline (pNA) after cleavage from the labeled substrate DEVD-pNA. For this, 1×10^6 cells/ml were seeded in a T75 cm^3 culture flask and treated 24 h after with the retained compounds at their respective efficacy concentrations for 48 h. Thereafter, the cells were lysed on ice and centrifuged (12,000 rpm at 4 °C for 20 min) to isolate proteins (supernatant). After measuring the protein concentration, 100 μL of proteins in 50 μL were transferred onto a 96-well plate and diluted with 50 μL of 2 × Reaction buffer containing 10 mM of DTT. Then, 5 μL of the 4 mM DEVD-pNA substrate was added to each well and incubated (5% CO_2, 37 °C) for 2 h. The pNA light emission was quantified at 405-nm using a microplate TECAN reader.

2.3.7. Expression of cell signaling proteins

Sufficient number of cells were grown in culture flasks filled with RPMI 1640 and treated with retained compounds at their respective efficacy concentrations for 48 h. Lysing and centrifugation of the cells were done at 14,000 rpm/10 min at 4 °C to extract proteins. After measuring the protein concentration, they were separated by electrophoresis at 120 V (400 mA, 150 W) for 90 min using a 10% NuPAGE Bis-Tris Plus Gel of 10 wells. Thereafter, the proteins were blotted onto nitrocellulose membranes (115 V, 115 mA, 150 W, 75 min), which were blocked for nonspecific proteins with Tris buffer containing tween and 10% skimmed milk for 1 h. The membranes were then incubated with pAKT (IgG1, monoclonal, dilution 1:2000), AKT (IgG1, monoclonal, dilution 1:1000), pmTOR (IgG1, monoclonal, dilution 1:1000), mTOR (IgG1, monoclonal, dilution 1:1000), VEGF (IgG1, monoclonal, dilution 1:1000), ZO-1 (IgG1, monoclonal, dilution 1:1000), β-Catenin (IgG1, dilution 1:1000), N-Cad (IgG1, dilution 1:1000), vimentin (clone D21H3, dilution 1:1000) and β-actin (1:20,000) at 4 °C for 24 h; all from Invitrogen or BD Biosciences (Heidelberg, Germany). The secondary antibodies used in this study were HRP (Horseradish peroxidase)-conjugated goat anti-mouse IgG (Upstate Biotechnology, Lake Placid, NY, USA; dilution 1: 5000) or anti rabbit IgG, respectively, for 1 h. The membranes were briefly incubated with ECL (Enhanced chemiluminescence) detection reagent (ECLTM, Amersham/GE Healthcare, Munich, Germany) to visualize the proteins and then analyzed by the

Fusion FX7 system (Peqlab, Erlangen, Germany). β-actin served as the internal control.

2.4. Assessment of anti-metastatic potential

2.4.1. Wound-healing assay

This assay assesses the inhibition of PC3 cell migration in the presence of isolates (**2** and **10**). The cells were seeded on 6-well plates at 5 × 10^5 cells/well and left to grow until confluence. Four hours before the creation of the wound, the medium was replaced by a serum-free RPMI 1640 medium. Furthermore, a scratch wound was created using a 100 µL pipette tip and then washed twice with PBS to remove mechanically detached cells. Compounds or control solvent (DMSO) were added in serum-free RPMI 1640 medium and cells were allowed for 72 h. The variation in recovery of the wounded area by migrating cells was recorded under a fluorescent microscope (10 ×) Olympus CK2/ULWCCD 0.030 (Olympus, Japan). Microphotographs were taken every 24 h and the area of wound healing was evaluated using ImageJ ® software.

2.4.2. Chemotaxis assay

Serum-induced cell migration was assessed using 6-well transwell chambers (Greiner, Frickenhausen, Germany) equipped with 8 µm pores. PC3 cells were seeded into the upper chamber and incubated for 24 h in serum-free RPMI 1640 medium, while the lower chamber contained RPMI 1640 supplemented with 10% serum. Following the 24-h incubation period, non-migrating cells on the upper surface of the transwell membranes were gently removed using a cotton swab. Cells that had migrated to the lower surface of the membrane were then stained with hematoxylin and counted separately under an Olympus microscope.

2.4.3. Cell adhesion to extracellular matrix components assay

Six-well plates pre-coated with extracellular matrix collagen or fibronectin were used. PC3 cells were exposed to the respective effective concentrations of compounds for 48 h in T25 cm^3 culture flasks. The plates, whether plastic or coated with collagen or fibronectin, were incubated with 1% bovine serum albumin (BSA) in phosphate-buffered saline (PBS) for 1 h at room temperature to prevent nonspecific cell adhesion. Subsequently, 1 × 10^5 treated or untreated (control) cells were added to each well and allowed to adhere for 60 min. After that, non-adherent cells were washed off with PBS, and the adherent cells were fixed with 1% glutaraldehyde. Cell counts were performed in five different fields using an Olympus microscope (20 × objective) to determine the average cellular adhesion rate.

2.5. Statistical analysis

Data analysis was performed using GraphPad Prism software version 5.00. Each experiment was replicated at least three times to ensure accuracy and reliability. Analysis of data involving three or more groups with a single variable was done using ANOVA, followed by Dunnett's post-hoc test for multiple comparisons. Statistical significance was established at a *p*-value less than 0.05.

3. Results

3.1. Structural elucidation of new compounds

3.1.1. Kerstingilactone (3)

White powder; IR (KBr) ν_{max} $cm^{-1:}$ 1017, 1141, 1159, 1230, 1513, 2854, 2893, 2938 and 2973; UV λ_{max} nm: 208, 230 and 278; HR-LD^+-QTOF-MS m/z 409.1627 $[M+Na]^+$, calcd. for $C_{22}H_{26}NaO_6$ 409.1627; ^1H NMR (600 MHz, CD_3OD) and ^{13}C NMR (150 MHz, CD_3OD) data see Table 1.

Compound **3** was obtained as a white powder from the ethyl acetate extract of leaves using the hexane-ethyl acetate (95/05) elution system. On its HR-LD^+-QTOF-MS spectrum (Fig. S2), the peak of the pseudo molecular ion is observed at $[M+Na]^+$ at m/z 409.1627, corresponding to the molecular formula $C_{22}H_{26}O_6$ with 10 degree of unsaturation. Its IR spectrum (Fig. S3) reveals the vibrations of methyl groups at, ν_{max} 2854, 2893, 2938, and 2973 cm^{-1} of carbonyl function at ν_{max} 1752 cm^{-1}, and for aromatic C=C band at 1510 cm^{-1}. Aromatic characteristic wave lengths are observed at 208, 230 and 278 nm on its UV spectrum (Fig. S4).

Table 1
^1H (600 MHz), ^{13}C (150 MHz) NMR and HMBC data of kerstingilactone (**3**) in MeOD [δ (ppm), *J* (Hz)].

Position	$\delta^{13}C$ (ppm)	HSQC	HMBC	COSY
1	180.1	–		
2	37.6	2.59 (m, 2H)		
3	34.0	2.94 (dd, J = 14.0, 5.3 Hz, 1Hα)	C-5; C-1′; C-6'; C-1	Hβ
		2.85 (dd, J = 14.0, 7.4 Hz, 1Hβ)		Hα
4	46.3	2.71 (dt, J = 7.7, 5.5 Hz, 1H)		
5	41.1	2.55 (dt, J = 14.4, 5.5 Hz 1H)		
6	71.5	4.21 (dd, J = 8.9, 7.4 Hz, 1Hα)		
		3.97 (dd, J = 9.0, 7.6 Hz, 1Hβ)		
1′	130.8	–		
2′	112.8	6.73 (d, J = 2.0 Hz, 1H)	C-6′; C-3′	
3′	149.1	–		
4′	147.9	–		
5′	111.5	6.85 (d, J = 8.1 Hz, 1H)	C-4′; C-1′	
6′	121.4	6.69 (dd, J = 8.1, 2.0 Hz, 1H)		
1″	131.8	–		
2″	112.2	6.62 (d, J = 2.0 Hz, 1H)	C-6″; C-3″	
3″	149.0	–		
4″	147.8	–		
5″	111.6	6.84 (d, J = 8.0 Hz, 1H)	C-4″; C-1″	
6″	120.6	6.63 (dd, J = 8.0, 2.0 Hz, 1H)		
1‴	55.1	3.77 (s, 3H)	C-3′	
2‴	55.1	3.82 (s, 3H)	C-4′	
1⁗	54.9	3.79 (s, 3H)	C-3″	
2⁗	55.0	3.81 (s, 3H)	C-4″	

On the ^1H NMR spectrum (Fig. S5) of compound **3**, aromatic protons appear in the deshielded zone and coupled in two ABC systems at δ_H 6.73 (d, J = 2.0 Hz, H-2′), δ_H 6.85 (d, J = 8.1 Hz, H-5′), δ_H 6.69 (dd, J = 8.1, 2.0 Hz, H-6′), δ_H 6.62 (d, J = 2.0 Hz, H-2″), δ_H 6.84 (d, J = 8.0 Hz, H-5″) and δ_H 6.63 (dd, J = 8.0, 2.0 Hz, H-6″), suggesting the presence of two aromatic rings substituted in the same manner. This suggests the quasi-symmetric nature of compound **3**. On the same spectrum, other signals are observed at δ_H 4.21 (dd, J = 8.9, 7.4 Hz, H-6α) and at δ_H 3.97 (dd, J = 9.0, 7.6 Hz, H-6β) corresponding to two diastereotopic protons of an oxymethylene unit related to a carbonyl group; at δ_H 2.94 (dd, J = 14.0, 5.3 Hz, H-3 α), δ_H 2.85 (dd, J = 14.0, 7.4 Hz, H-3β) and at δ_H 2.59 (m, H-2) corresponding to 4 diastereotopic protons of two methylene groups with one directly linked to a carbonyl group. Signals of two protons of methines linked to the aromatic ring are also observed on this spectrum at δ_H 2.71 (1H, dt, J = 7.7, 5.5 Hz, H-4) and at δ_H 2.55 (1H, dt, J = 14.4, 5.5 Hz, H-5) the couplage constance of 5.5 Hz observed between H-4 and H-5 allowed us to think that those two proton are *cis* together. Signals of protons of four methoxy groups are observed at δ_H: 3.82, 3.81, 3.79 and 3.77 ppm. All these observed signals suggest that compound **3** is a lactone with two aromatic rings.

The totally decoupled ^{13}C NMR spectrum (Fig. S7) of compound 3 presents signals of 22 carbons attributable according to its DEPT 135 experiment (Fig. S7), to four primary carbons of the methoxy group at:

δ_C 55.1 (C-1‴ and C-2‴), δ_C 54.9 (C-1⁗) and δ_C 55.0 (C-2⁗). Three secondary carbons of two methylene groups (37.6 (C-2) and δ_C 34.0 (C-3)); and of one oxymethylene group (δ_C 71.5 (C-6)). Eight tertiary carbons with two of the lactonic methines at δ_C 46.3 (C-4); δ_C 41.1 (C-5), and six of aromatic methines at δ_C: 112.8 (C-2′), 111.5 (C-5′), 121.4 (C-6′), 112.2 (C-2″), 111.6 (C-5″) and 120.6 ppm (C-6″). Seven quaternary carbons; two normal aromatics at δ_C 130.8 (C-1′) and δ_C 131.8 (C-1″); four oxy-quaternary aromatics at: δ_C 149.1 (C-3′), δ_C 147.8 (C-4′), δ_C 149.0 (C-3″) and δ_C 147.8 (C-4″) indicating that the four methoxy groups are in the *ortho* position on the two aromatic rings, and one quaternary carbon of the lactone carbonyl δ_C 180.1 (C-1). The HMBC (Fig. S9) analysis of compound 3 also facilitated the determination of the various linkages between the atoms indicated in Fig. S1. Important correlations are observed between H-3β and C-1′ (130.8), C-5 (41.1); between H-3α and C-1 (180.1); between H-2′ and C-3′ (149.1), C-6′ (121.4); between H-5′ and C-1′ (130.8), C-4′ (147.9); between H-2″ and C-3″ (149.0), C-6″ (120.6) between H-5″ and C-1″ (131.8); C-4″ (147.8), between methoxy protons at δ_H 3.77 and C-3′ (149.1); at δ_H 3.82 and C-4′ (147.9); at δ_H 3.79 and C-3″ (149.0); and at δ_H 3.81 and C-4″ (147.8). These four last observed correlation allowed us to situate methoxy groups in *ortho* position on the two aromatic rings (Table 1). From the above analysis the structure of compound **3** was determined as 5,6-bis(3,4-dimethoxyphenyl)oxepan-2-one a new phenolic lactone derivative trivially named kerstingilactone.

3.1.2. *Kerstinginone (**10**)*

Amorphous yellow powder; IR (KBr) ν_{max} $cm^{-1:}$ 1101, 1135, 1305, 1457, 1644, 1677, 2474, 2957 and 3339; UV λ_{max} nm: 211, 223,260, 268, 296 and 308; HR-LD$^+$-QTOF-MS m/z 379.1176 $[M+Na]^+$, calcd. for $C_{20}H_{20}NaO_6$ 379.1158; ^{1}H NMR (600 MHz, CD_3OD) and ^{13}C NMR (150 MHz, CD_3OD) data enclosed in Table 2.

Compound **10** was obtained as a yellow powder, soluble in methanol, with a melting point between 204 and 206 °C. The HR-LD$^+$-QTOF-MS spectrum (Fig. S11) exhibits the pseudo molecular ion $[M+Na]^+$ at m/z 379.1176, which is in accordance with the molecular formula $C_{20}H_{20}O_6$ containing 6 degrees of unsaturation. Its IR spectrum (Fig. S12) reveals the vibrations of the hydroxy function at, ν_{max} 3339 cm^{-1}, two carbonyl functions at ν_{max} 1644 cm^{-1} and ν_{max} 1677 cm^{-1} and for aromatic C=C band at 1462 and 1505 cm^{-1}. Aromatic characteristic wavelengths are observed at 225, 265 and 290 nm on its UV spectrum (Fig. S13).

In the ^{1}H RMN spectrum (Fig. S14) of compound 10, four olefinic signals are observed at δH 7.20 (*d*, $J = 10.3$ Hz; H-2′); 6.58 (*d*, $J = 9.5$; H-1″), 6.06 (d, $J = 10.3$ Hz; H-3′) and 5.58 (*d*, $J = 9.5$; H-2″). The δH value of H-2′ indicates that one double bond is conjugated with a carbonyl group. Coupling constants: $J = 10.3$ Hz and $J = 9.5$ Hz show that H-2′ and H-3′ in the same way as H-1″ and H-2″ are coupling together. This hypothesis is confirmed by the COSY spectrum (Fig. S18) of compound **10,** on which correlations are observed between H-2′ and H-3′; and between H-1″ and H-2″. One aromatic proton is observed at δH 5.94 (s; H-8) on the same spectrum and suggest that the aromatic ring is penta-substituted. Two characteristic signals of the C ring of flavanone are also observed on this spectrum at δ_H 2.72 (dd; $J_1 = 3.0$ Hz; $J_2 = 17.1$ Hz, H-3a); δ_H 3.08 (dd; $J_3 = 13.4$ Hz; $J_2 = 17.1$ Hz, H-3b) and at δ_H 4.54 ppm (dd; $J_1 = 3.0$ Hz; $J_3 = 13.4$ Hz, H-2) (Yenesew et al., 1998). According to previous works, J_1 (3.0 Hz) and J_3 (13.4 Hz) coupling constance of H-2 are in accordance with a 2*S* flavanone (Yenesew et al., 1998; Promsattha et al., 1986). Four signals of diastereotopic protons are observed at δ_H 2.69 (1H, ddd; $J = 17.3$; 8.8; 5.4 Hz, $H_{5'\alpha}$), 2.54 (1H, ddd; $J = 17.3$; 8.8; 5.4 Hz, $H_{5'\beta}$), 2.11 (1H, ddd; $J = 13.9$; 9.2; 4.9 Hz, $H_{6'\alpha}$) and at 2.24 ppm (1H, ddd; $J = 13.9$; 9.2; 4.9 Hz, $H_{6'\beta}$), suggesting that the B ring of this flavanone has been reduced (Table 2). Two signals of methyl protons are also observed on this spectrum at δ_H 1.44 (s; 3H) and δ_H 1.42 (s; 3H).

The completely decoupled ^{13}C NMR spectrum (Fig. S16) of compound **10** presents 20 carbon signals which were identified based on the analysis of its DEPT 135 spectrum (Fig. S16): three secondary carbons at δ_C 31.3 (C-6′), 33.1 (C-5′), and 35.5 ppm (C-3); six tertiary carbons including the characteristic one on flavanone at δ_C 82.0 ppm (C-2); this value is also in accordance with a 2*S* flavanone (Yenesew et al., 1998; Promsattha et al., 1986); four of the two olefinic double bond at δ_C 149.6 (C-2′), 129.1 (C-3′), 126.2 (C-2″) and 114.6 (C-1″) with the one at 149.6 ppm confirming that one of the double bonds is conjugated to one carbonyl group; and one aromatic methine at 95.4 ppm (C-8). Two primary carbons, simple substitutions of methyl, are at δ_C 27.2 (C- 4″) and 27.1 ppm (C-5″). Nine quaternary carbons are deduced including two conjugated ketones at δ_C 199.6 (C-4′) and 196.5 ppm (C-4); five hybridized sp2 quaternary carbons at δ_C 162.1 (C-7), 161.7 (C-5), 157,1 (C-9), 102.7 (C-10) and 102.2 ppm (C-6); two hybridized sp^3 quaternary carbons at δ_C 69.2 ppm (C-1′) and δ_C 78.0 ppm (C-3‴).

Many correlations between protons and carbons have been observed in the HMBC spectrum (Fig. S17) of compound **10**. These correlations allowed to locate carbonyls, hydroxy and other substituents on compound **10**. Important correlations are observed between the proton at δ_H 5.95 (H-8) and carbons at δ_C 162.1 (C-7) and 102.7 ppm (C-10); between the proton at δ_H 6.58 (H-1″) and carbons at δ_C 161.7 (C-5), 102.2 (C-6) and 78.0 ppm (C-3‴); between the proton at δ_H 5.58 (H-2″) and carbons at δ_C 102.2 (C-6), 78.0 ppm (C-3‴), and 27.2 (C- 4″); between the proton at δ_H 7.21 (H-2′) and carbons at δ_C 199.6 (C-4') and 31.3 (C-6′) and between the proton at δ_H 6.06 (H-3′) and carbons at δ_C 69.2 ppm (C-1′) and at 33.1 (C-5′). All of these correlations are shown in Fig. S11. Based on the above analysis the structure of compound **10** was determined as 5-hydroxy-2*S*-(1′-hydroxy-4′-oxocyclohex-2′-en-1′*S*-yl)-3‴,3‴-dimethyl-2,3-dihydropyrano [3,2-*g*]chromen-4(8*H*)-one a new flavanone derivative trivially named kerstinginone (see Fig. 1).

Table 2
^{1}H (600 MHz), ^{13}C (150 MHz) NMR and HMBC data of kerstinginone (**10**) in MeOD [δ (ppm), *J* (Hz)].

Position	δ^{13}C (ppm)	HSQC	HMBC	COSY
2	82.0	4.54 (1H, dd; *J1* = 3.0; *J3* = 13.4 Hz)	C-5	H_β −3
3	35.5	2.72 ($1H_\alpha$, dd; *J1* = 3.0; *J2* = 17.1 Hz)	C-4; C-10	–
		3.08 ($1H_\beta$, dd; *J3* = 13.4; *J2* = 17.1 Hz)	C-1′; C-2; C-4	H-2
4	196.5	–	–	–
5	161.7	–	–	–
6	102.2	–	–	–
7	162.1	–	–	–
8	95.4	5.94 (1H, s)	C-6; C-5; C-4	–
9	157,1	–	–	–
10	102.7	–	–	–
1′	69.2	–	–	–
2′	149.6	7.20 (1H, *d*, *J* = 10.3 Hz)	C-4′; C-2; C-6′	H-3′
3′	129.1	6.06 (1H d, *J* = 10.3 Hz)	C-5′; C-1′	H-2′
4′	199.6	–	–	–
5′	33.1	2.69 (1H, m) 2.54 (1H, m)	C-6′; C-1′; C-4′	–
6′	31.3	2.11 (1H, m) 2.24 (1H, m)	C-5′; C-2; C-2′; C-4′	–
1″	114.6	6.58 (1H, *d*, *J* = 9.5)	C-7; C-6; C-3″	H-2″
2″	126.2	5.58 1H, *d*, *J* = 9.5)	C-6; C-3″; C-4″; C-5″	H-1″
3″	78.0	–		–
4″	27.2	1.42 (3H, s)	C-5″; C-3″; C-2″	–
5″	27.1	1.44 (3H, s)	C-4″; C-3″; C-2″	–

3.2. *Antiproliferative activity*

3.2.1. *Effect of crude extracts on prostate cancer cell growth*

The ethanolic extract of *C. kerstingii* leaves (CKL-EE) significantly ($p < 0.001$) reduced the growth of androgen-sensitive (LNCaP) and androgen non-sensitive (PC3) cells at the tested concentrations (Fig. 2A and B).

The ethyl acetate crude extract of *C. kerstingii* leaves (CKL-EA)

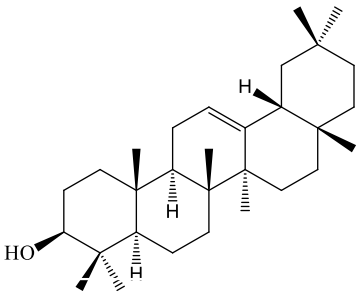

1 (3-hydroxyolean-12-ene)

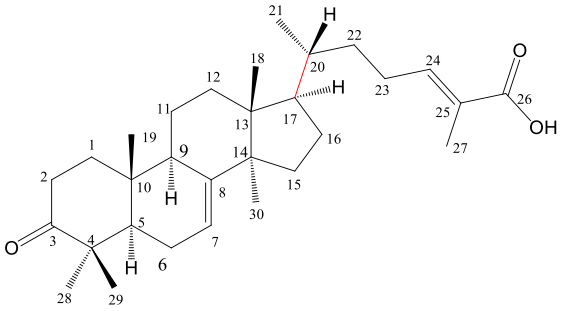

2 (Masticadienonic Acid)

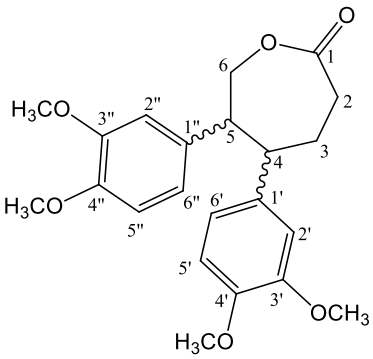

3 (kerstingilactone)

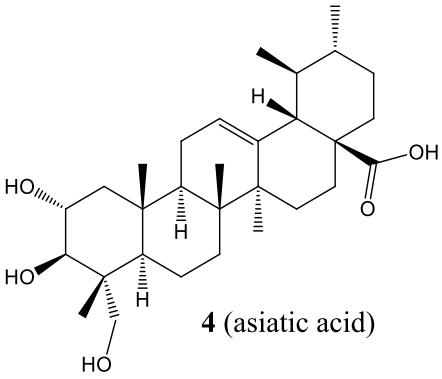

4 (asiatic acid)

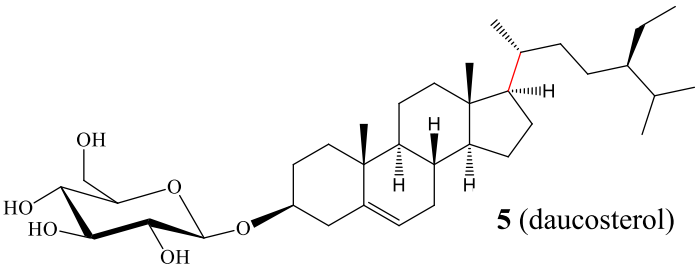

5 (daucosterol)

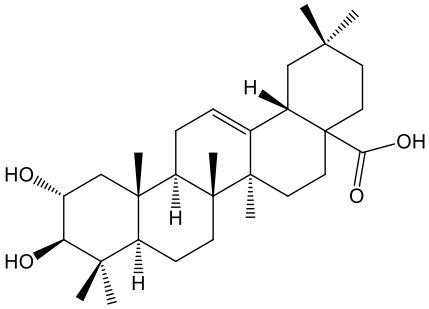

6 (2,3-dihydroxyolean-12-en-oic acid)

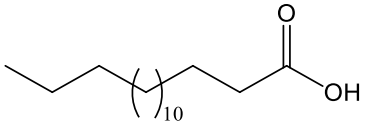

7 (palmitic acid)

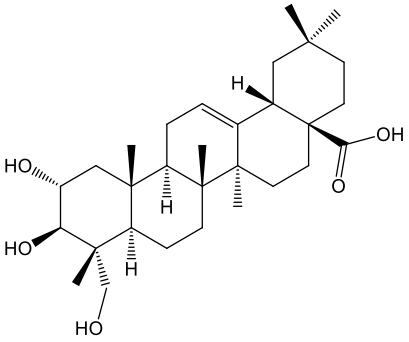

8 (5,6-dihydrobassinic acid)

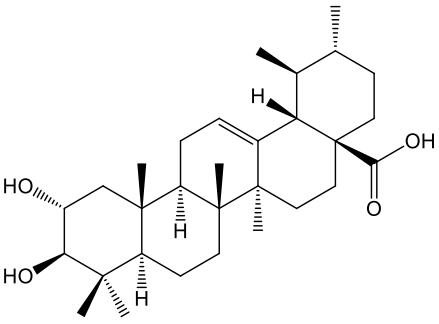

9 (2,3-dihydroxyurs-12-en-oic acid)

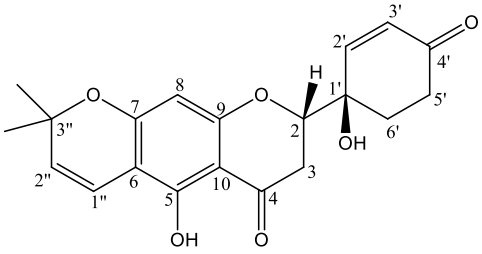

10 (kerstinginone)

Fig. 1. Isolated compounds (1–10) from leaves and stem barks of *Commiphora kerstingii*.

significantly ($p < 0.001$) inhibited LNCaP cell growth at all the tested concentrations (Fig. 2C), while it induced a concentration-dependent decrease in PC3 cells at 12.5 and 50 μg/mL ($p < 0.01$) and 200 μg/mL ($p < 0.001$) (Fig. 2D) (see Fig. 1).

The ethyl acetate (CK-EA) and ethanolic (CK-EE) crude extract of *C. kerstingii* stem barks showed strong inhibition ($p < 0.001$) of LNCaP cells at all tested concentrations (Fig. 2E and G), while PC3 cell growth arrest was concentration-dependent ($p < 0.01$ at 12.5 and 50 μg/mL and

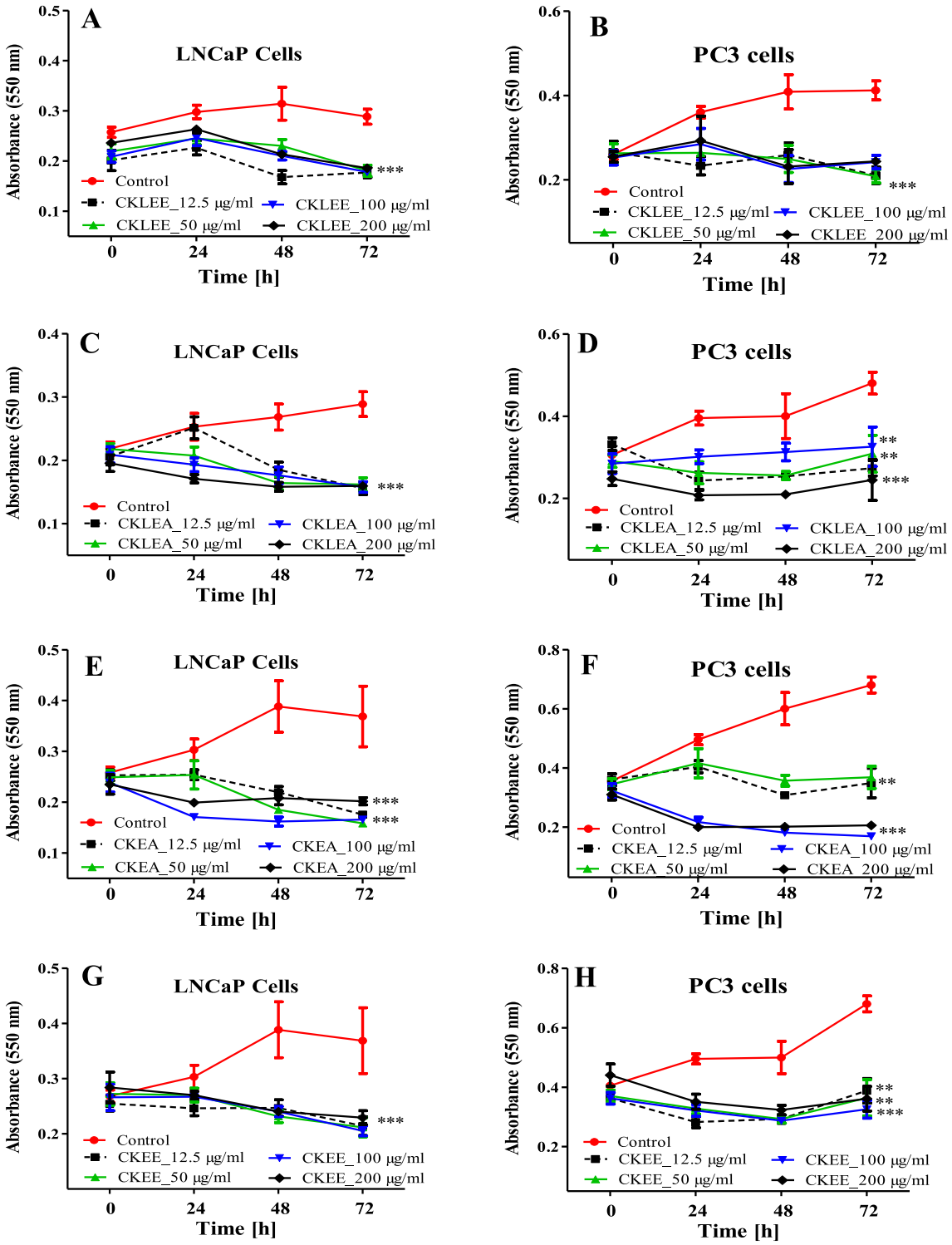

Fig. 2. Growth of androgen sensitive LNCaP (A, C, E & G) and non-sensitive PC3 (B, D, F & H) prostate carcinoma cells treated with different concentrations (12.5–200 µg/mL) of compounds the ethanolic (CKL-EE) and ethyl acetate (CKL-EA) extract of *C. kertingii* leaves as well as the ethyl acetate (CK-EA) and ethanolic (CK-EE) crude extract of *C. kertingii* stem barks after 24, 48 and 72 h. Controls remained untreated. (n = 3). Treated cancer cell cultures were compared to non-treated control cultures of the same passage and cell numbers per well. $^{**}p < 0.01$ and $^{***}p < 0.001$ compared to control.

$p < 0.001$ at 100 and 200 µg/mL) following exposure to these extracts (Fig. 2F and H).

3.2.2. *Effect of compounds on prostate cancer cell growth*

Fig. 3 depicts that out of the 10 tested compounds isolated from leaves and stem bark extracts of *C. kerstingii*, two compounds, namely kerstinginone (**10**), a new flavanone and Masticadienonic Acid (**2**), exhibited promising cytotoxic effects.

Since compounds **10** (new compound) and **2** showed better cytotoxic potential, they were further tested for their capability to inhibit cell growth. Compound **2** showed significant and concentration-dependent inhibition of PC3 cells ($p < 0.01$ at 5 µg/mL and $p < 0.001$ at 10, 20

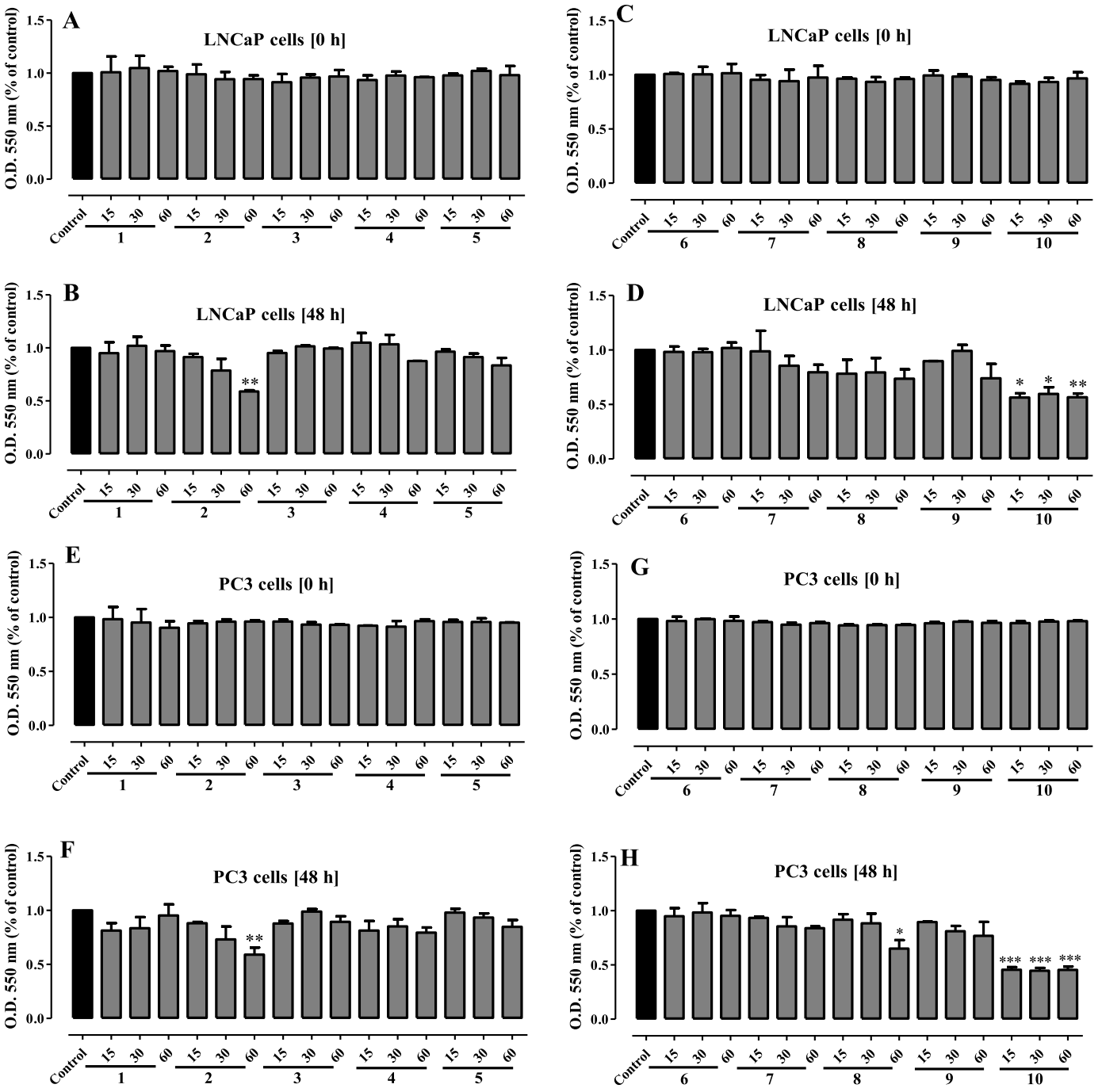

Fig. 3. Screening of the 10 compounds from *Commiphora kerstingii* for their potential cytotoxic effect. LNCaP (A to D) and PC3 (E to H) cancerous cells were treated for 48 h with compounds at concentrations of 15, 30 and 60 μg/mL and MTT assay was performed at 0 h and 48 h $^{*}p < 0.05$, $^{**}p < 0.01$ and $^{***}p < 0.001$ compared to control.

and 40 μg/mL) but only impacted the growth of LNCaP at the concentration of 40 μg/mL ($p < 0.05$) compared to control cells (Fig. 4A & B). The magnitude of growth suppression induced by compound **10** was strong and increased with time, at optimal concentrations of 2.5–10 μg/mL (Fig. 4C–D).

As expected, the standard (docetaxel) induced a strong inhibition of PC3 and LNCaP cells in a concentration-dependant effect, with the maximum effect at 1 μM (Fig. 4 E & F).

3.2.3. *Effect of compounds on cell proliferation and clone formation*

Fig. 5 depicts the effects of compounds **2** and **10** on prostate cancer cell proliferation. A significant inhibition ($p < 0.05$) of cell proliferation was observed with compound **2** in PC3 and LNCaP cells (except for the concentration of 5 μg/mL) (Fig. 5A–B). Moreover, Compound **10** induced a potent inhibition of PC3 and LNCaP cell proliferation rate at 1.25 ($p < 0.05$), 2.5 ($p < 0.001$) and 5 μg/mL ($p < 0.001$) after a 48 h treatment (Fig. 5B–D).

As far as the number of clones formed is concerned (Fig. 5E–F), a significant and concentration-dependent inhibition ($p < 0.001$) of PC3 clone formation was observed with both compounds **2** and **10** at tested concentrations: 5, 10 and 20 μg/mL for compound **2** and 1.25, 2.5 and 5 μg/mL for compound **10**.

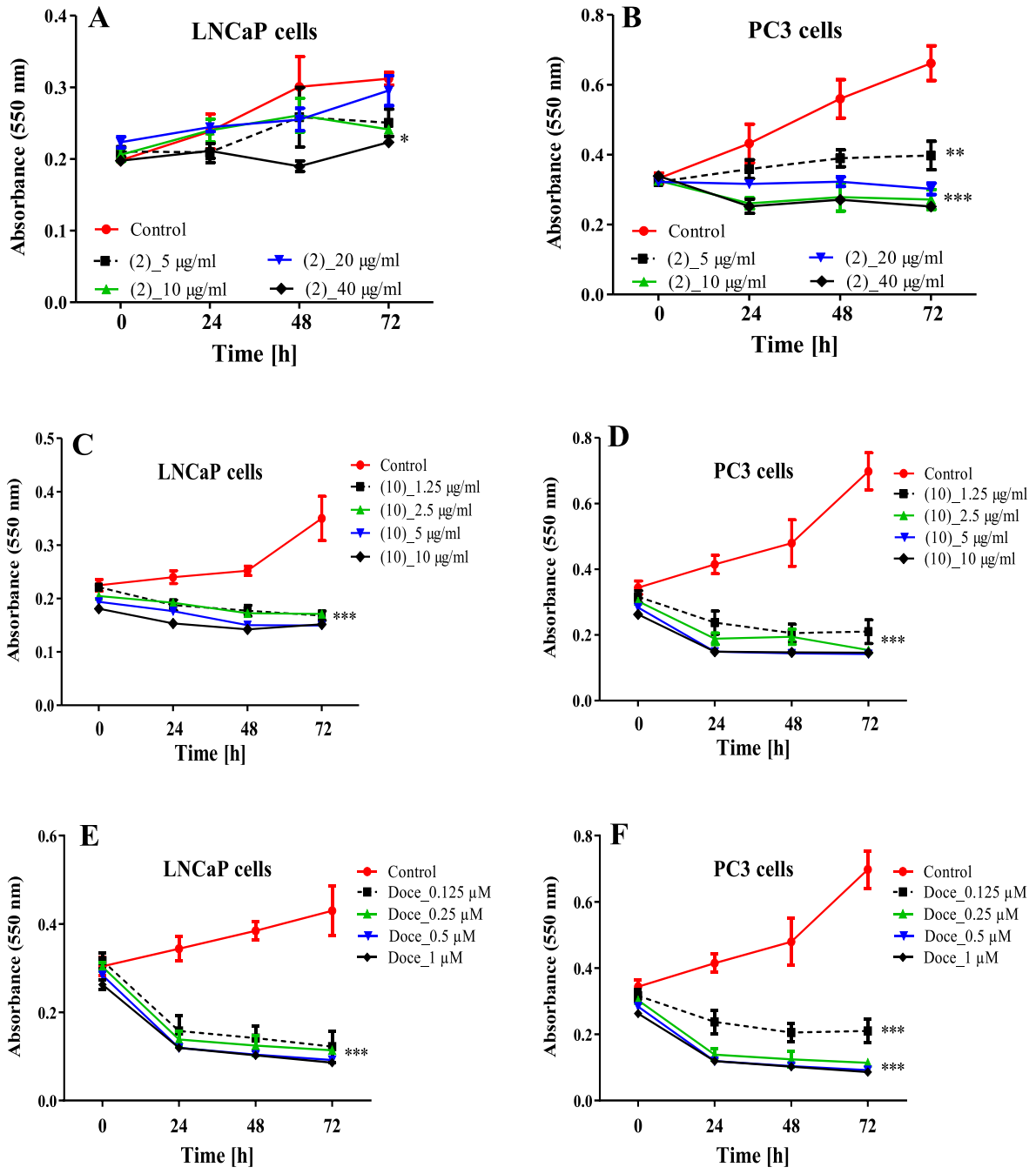

Fig. 4. Growth of androgen sensitive LNCaP (A, C & E) and non-sensitive PC3 (B, D & F) prostate carcinoma cells treated with different concentrations of compounds **2** and **10** as well as docetaxel after 24, 48 and 72 h. Controls remained untreated. (n = 3). Treated cancer cell cultures were compared to non-treated control cultures of the same passage and cell numbers per well. *$p < 0.05$, **$p < 0.01$ and ***$p < 0.001$ compared to control.

3.2.4. Effect of compounds on apoptosis and caspase-3 assay

Compound **2** induced an increment in apoptotic cell population (25%) only in LNCaP cells (Fig. 6A, 6 B and 6C). Fig. 6D–E shows that this was correlated with a slight increase in caspase activity ($p < 0.05$) at a concentration of 20 µg/mL in LNCaP cells.

As far as the compound **10** is concerned, it induced a potent apoptotic effect on both PC3 and LNCaP cells and this effect was concentration-dependent: 55% of apoptotic cells at a concentration of 5 µg/mL and 70% at 10 µg/mL (Fig. 7B–C). The caspase-3 activity also increased in both LNCaP and PC3 cells, although significant ($p < 0.001$) only at a concentration of 10 µg/mL.

3.2.5. Effect of compounds on cell migration

Compound **2** inhibited PC3 cell migration into the free zone at concentrations of 10 and 20 µg/mL after 48 and 72 h (Fig. 8). Compound **10** exhibited such an effect in PC3 cells at concentrations of 2.5 and 5 µg/mL after 72 h, while it failed to do so at 2.5 µg/mL after 48 h (Fig. 9). The concentration of 10 µg/mL killed cells in this system after 72 h.

3.2.6. Effect of compounds on cell invasion

The number of invading PC3 cells was significantly reduced following incubation with compound **2** (10 µg/mL, $p < 0.01$) or **10** (2.5 and 5 µg/mL, $p < 0.001$) (Figure 10A, 10 B and 10 C).

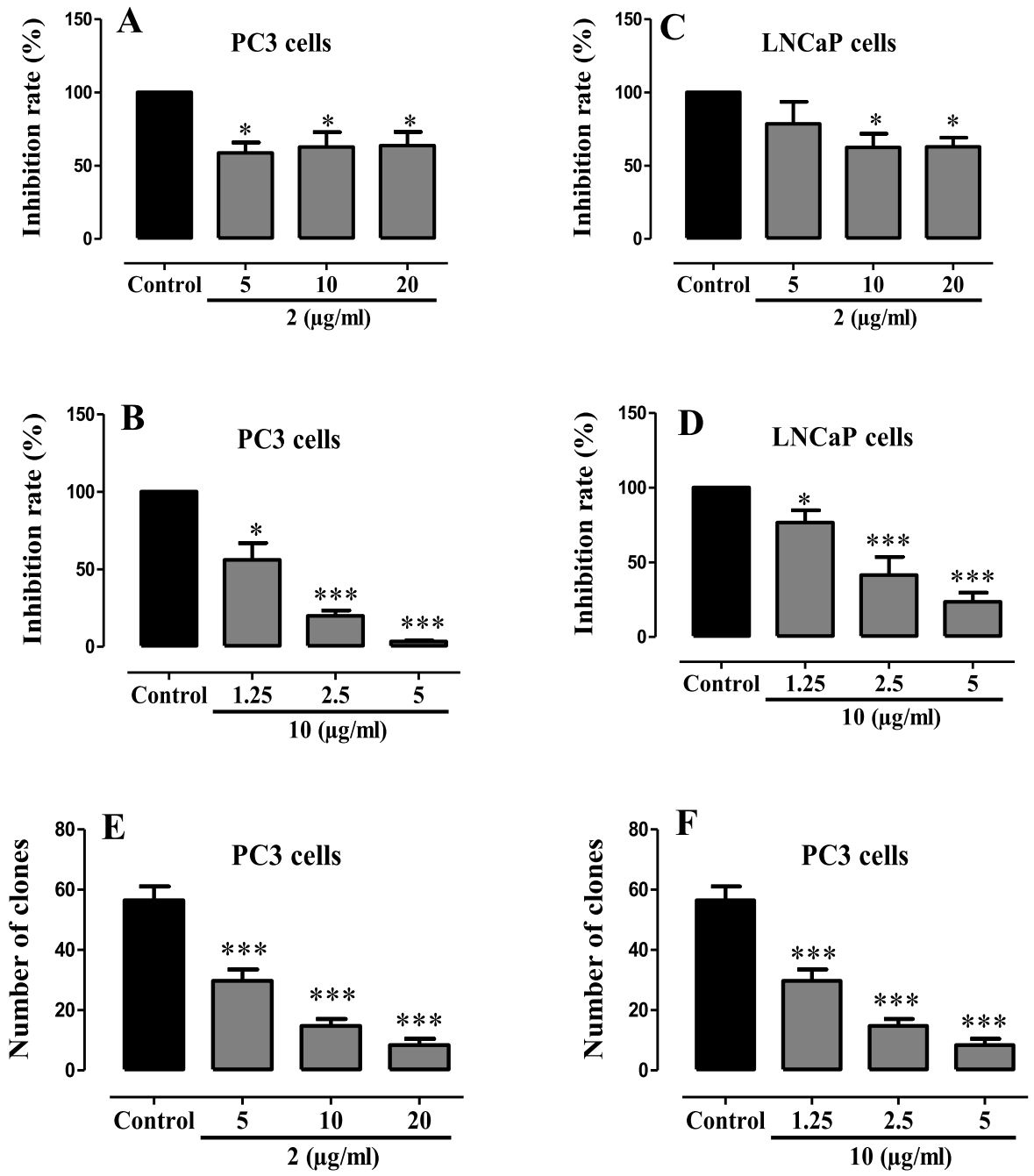

Fig. 5. Cell proliferation of LNCaP and PC3 cells treated with compounds **2** (A & C) at 5, 10 and 20 µg/mL and **10** at 1.25, 2.5 and 5 µg/mL (B & D), after 48 h. Clonogenic growth of PC3 cells exposed to compound **2** (E) at 5, 10 and 20 µg/mL and **10** (F) at 1.25, 2.5 and 5 µg/mL after 48 h. Control remained untreated. *$p <$ 0.05 and ***$p < 0.001$ compared to control.

3.2.7. Effect of compounds on cell adhesion

Compound **2** at 5 µg/mL increased cell adherence to both collagen ($p < 0.01$) and fibronectin ($p < 0.05$), while at 10 µg/mL it increased cell adherence only to collagen ($p < 0.05$) (Fig. 10D).

Compound **10** significantly ($p < 0.05$) increased the adherence of PC3 cells to fibronectin at 2.5 µg/mL (Fig. 10E).

3.2.8. Expression of some key proteins in cell proliferation and migration

Fig. 11 shows the expression of some proteins involved in cell signaling. A decrease in the expression of pAKT, AKT, VEGF (at 2.5 µg/mL) and N-cadherin was noticed following treatment with compound **10**, while the phosphorylated protein expression of mTOR, vimentin and β-catenin increased.

4. Discussion

Plant extracts have long been utilized for managing various ailments, as they offer a vast array of novel and bioactive chemical compounds for the development of chemotherapeutic agents. Many of these plant-derived compounds demonstrate favorable side effect and toxicity profiles compared to conventional chemotherapeutic agents. In the context of prostate cancer treatment, numerous plant species from families such as Annonaceae, Apocynaceae, Asteraceae, Combretaceae, Euphorbiaceae, Fabaceae, Lamiaceae, Malvaceae, Phyllantheraceae, Poaceae, Rutaceae, Solanaceae, and Zingiberaceae have exhibited considerable effects. However, research investigating the anticancer properties of species from the Burseraceae family, including *Commiphora kerstingii*

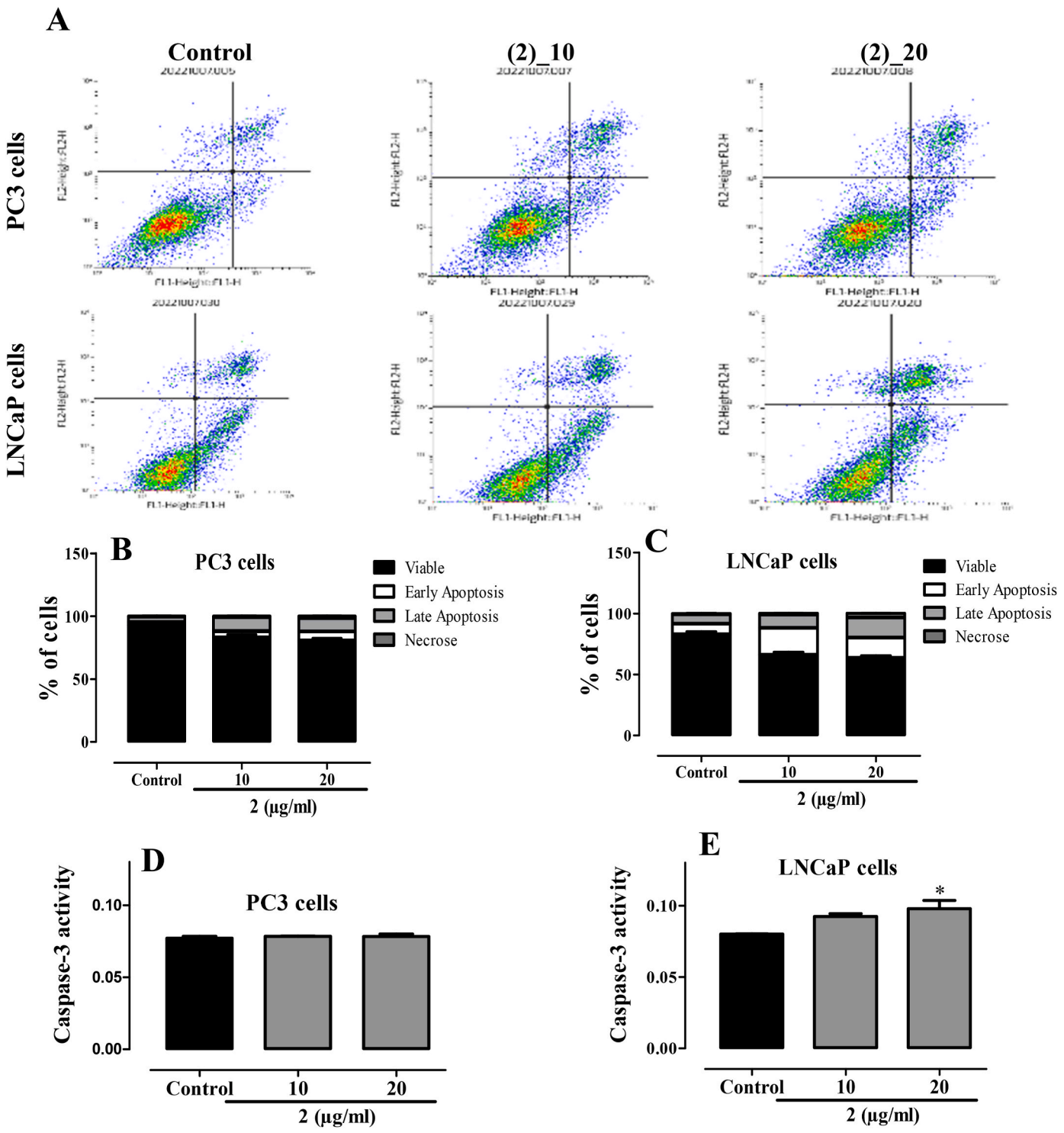

Fig. 6. Dotplots (A) and representative of apoptosis measurement by Annexin V-FITC/PI staining in PC3 (**B**), and LNCaP (**C**) cells after 48 h of pretreatment with compound **2** at final concentrations of 10 and 20 µg/mL. Caspase-3 activity of PC3 (**D**) and LNCaP (**E**) cells following 48 h pretreatment of subconfluent cultures with **2**. The graphs show the percentage of cells in each phase of three independent experiments. *$p < 0.05$ compared to control.

Engl, remains scarce. Therefore, the present study aimed to characterize the phytochemical compounds present *in Commiphora kerstingii* and evaluate their effects and underlying mechanisms on prostate cancer cells.

C. kerstingii (leaves and stem barks) ethanolic or ethyl acetate crude extracts all significantly ($p < 0.001$) inhibited the growth of androgen-sensitive (LNCaP) and non-sensitive (PC3) prostate cancer cells. However, the most potent cell growth inhibition was observed with the ethyl acetate stem bark extract, suggesting the presence of semi-polar ingredients with anticancer potential in this extract. Previous studies have revealed that this extract is rich in alkaloids, phenols, tannins, saponins and volatile oils; and endowed with antioxidant activity (Toma et al., 2016; Musa, 2008). Purification of the ethyl acetate extract from stem bark led to the isolation of four compounds: one fatty acid: **7**: palmitic acid (Ortega and Segura, 2021), two triterpenes: **8**: 5,6-dihydrobassinic acid (Zhang et al., 2014) and **9**: 2,3-dihydroxyurs-12-en-oic acid

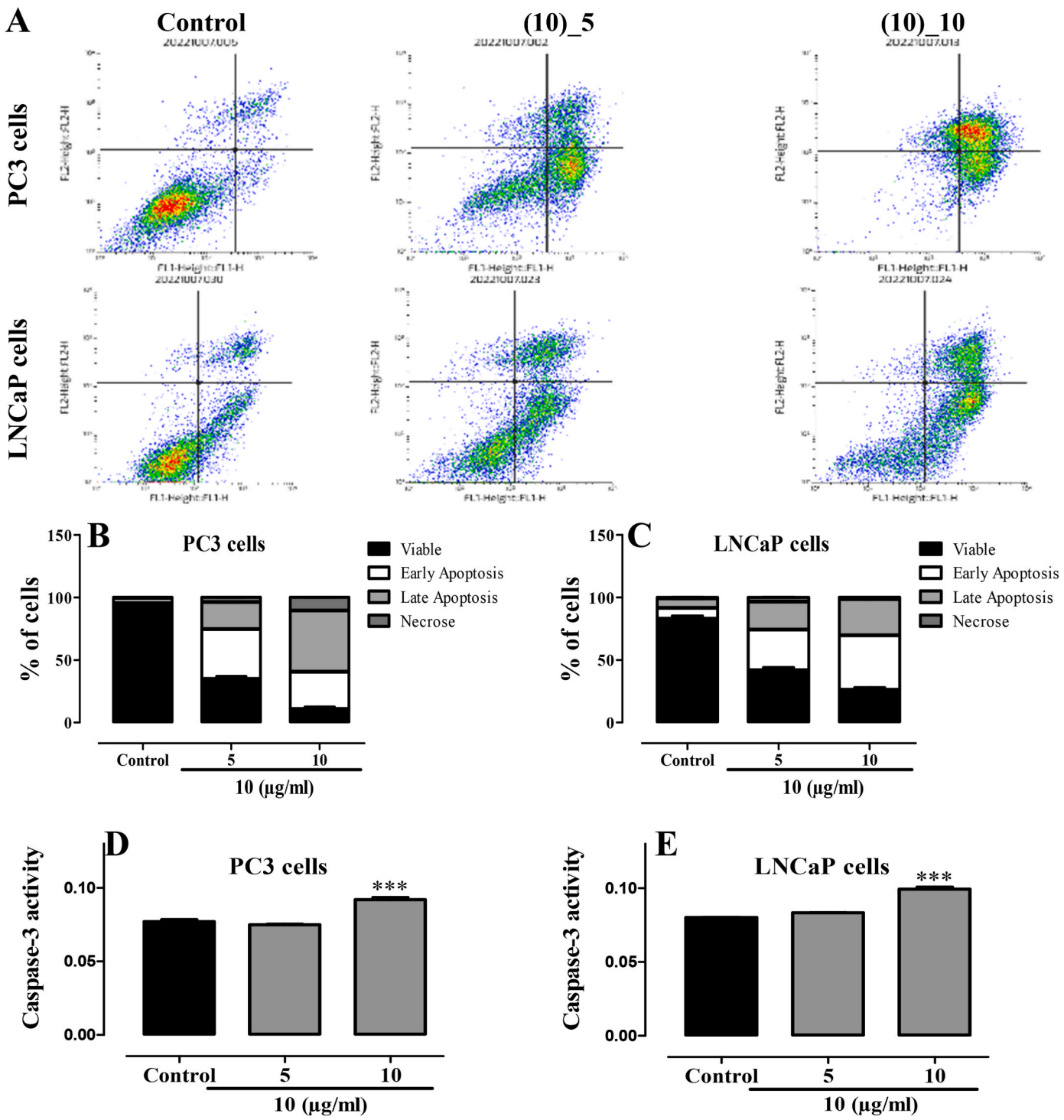

Fig. 7. Dotplots (**A**) and representative of apoptosis measurement by Annexin V-FITC/PI staining in PC3 (**B**), and LNCaP (**C**) cells after 48 h of pretreatment with compound **10** at final concentrations of 5 and 10 µg/mL. Caspase-3 activity of PC3 (**D**) and LNCaP (**E**) cells following 48 h pretreatment of subconfluent cultures with **10**. The graphs show the percentage of cells in each phase of three independent experiments. *$p < 0.001$ compared to control.

(Kazuyoshi et al., 1998) and one new flavanone derivative: **10**. From the ethyl acetate extract of leaves, six compounds were isolated, four triterpenes: **1**: 3-hydroxyolean-12-ene (Kazuyoshi et al., 1998), **2**: Masticadienonic Acid (Sara et al., 2021), **4**: asiatic acid (Kazuyoshi et al., 1998) and **6**: 2,3-dihydroxyolean-12-en-oic acid (Djoukeng et al., 2005); one sterol glucoside: **5**: Daucosterol (Yaya et al., 2018) and one new phenolic lactone derivative: **3**. Out of them, only compounds **2** and **10** exhibited significant arrest of cell growth. Interestingly, compound **10,** a new compound at optimal concentration of 2.5 µg/mL induced a strong and concentration-dependent inhibition of both LNCaP and PC3 cells. Compound **2** (Masticadienonic Acid) equally exhibited such effect, but at a lesser magnitude (10–20 µg/mL). The fact that they inhibit both androgen-sensitive and non-sensitive cells suggests that they might exert their action not only through androgen receptors mediated pathways but also through the inhibition of growth factor receptors such as Epidermal Growth Factor Receptor (EGFR), activation of tumor suppressor genes such as p53, p27, phosphatase and tensin homolog (PTEN), etc. (Jaglanian et al., 2020).

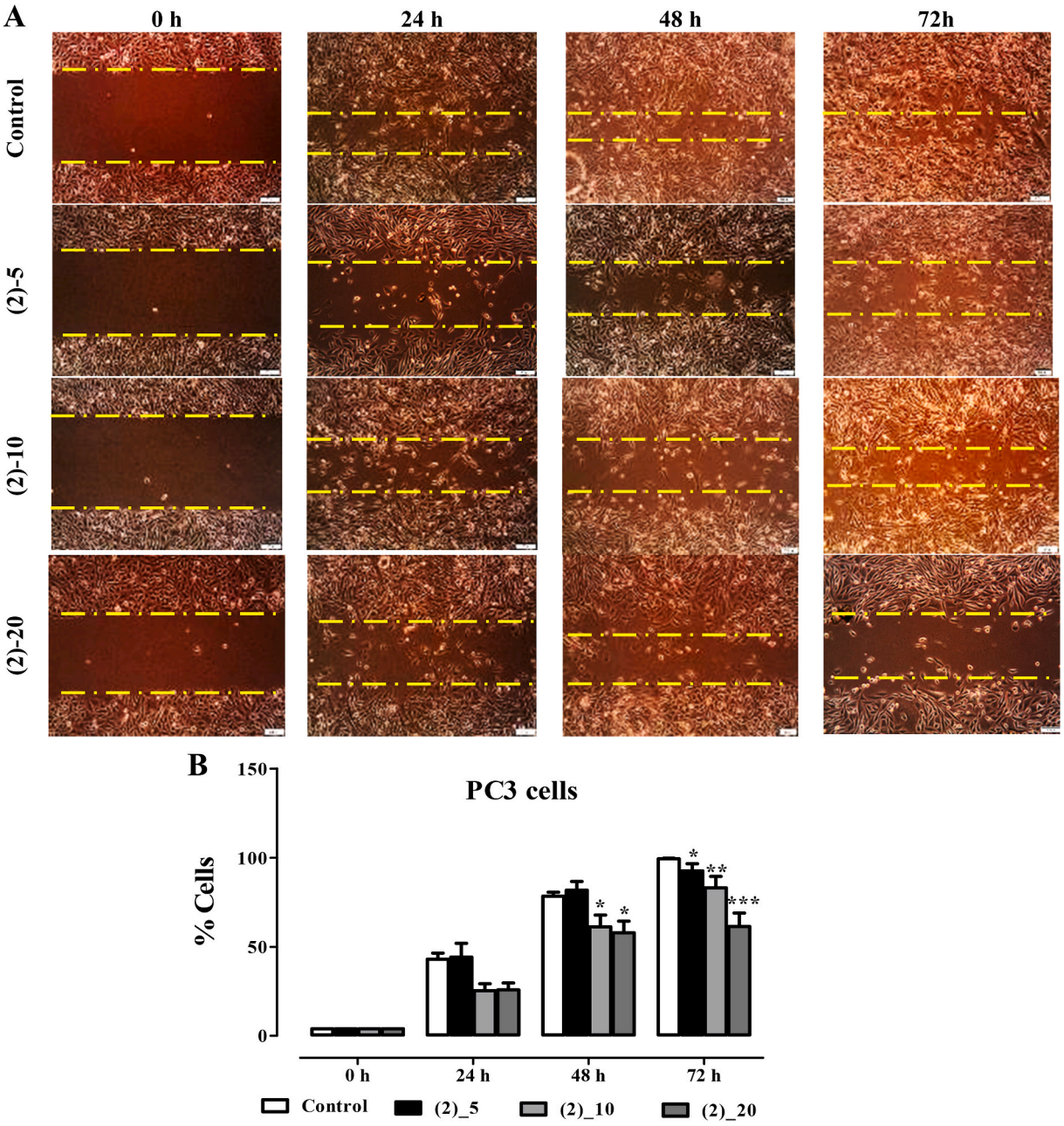

Fig. 8. Effects of compounds **2** on PC3 cells migration. Microphotographs of one assay (**A**) and graphic representation of three independent wound-healing assays (**B**) in PC3 cells migration after 72 h of treatment in serum free RPMI 1640 medium. $^{*}p < 0.05$, $^{**}p < 0.01$ and $^{***}p < 0.001$ as compared with control.

Apoptosis is one of the mechanisms most frequently used to evaluate the effect of natural products on the growth of cancer cells (Shishodia et al., 2007). The observed prostate cancer cell growth arrest could be due to the ability of compounds to induce programmed cell death or cause a cell cycle arrest. As shown in this study, compounds **2** and **10** were able to increase the percentage of apoptotic cells after treatment on LNCaP and PC3 cells, with the better effect being observed with compound **10**. This effect was positively associated with a significant ($p < 0.001$) increase in caspase 3 activity. Caspase 3 plays a critical role as a mediator in both the extrinsic and intrinsic pathways of apoptosis (Choi et al., 2016; Hussar, 2022). This implies that both compounds have the potential to induce apoptosis either through the mitochondrial pathway, involving mitochondrial membrane permeabilization, the release of apoptosome factors, and activation of caspases, or through the extrinsic pathway mediated by death receptors. The extrinsic pathway triggers the recruitment of adaptor proteins like Fas-associated protein with a death domain (FADD), subsequently recruiting downstream factors including caspase-8 and caspase 3. Additionally, both the newly identified flavanone **10** and Masticadienonic Acid **2** compounds significantly ($p < 0.001$) inhibited the formation of PC3 clones. This finding suggests that both compounds may disrupt the self-renewal capacity of PC3 prostate cancer cell lines, potentially by downregulating the expression of KLF4, Sox 2, and Oct 4 genes, or by targeting the Wnt signaling pathway, which is crucial for maintaining stemness (Soufi et al., 2012; Macfarlan et al., 2012; Cojoc et al., 2015).

Despite superior long-term survival in localized prostate cancer, metastasis characterized by cell motility and invasion remains a major problem even after intensive multimodal therapy. There is thus an urgent need to develop novel, effective strategies that prevent migration and invasion of cancer cells. In the present study, compound **10** at 2.5 and 5 μg/mL and compound **2** at 10 and 20 μg/mL inhibited prostate cancer migration after 48 h and 72 h of treatment. Both compounds

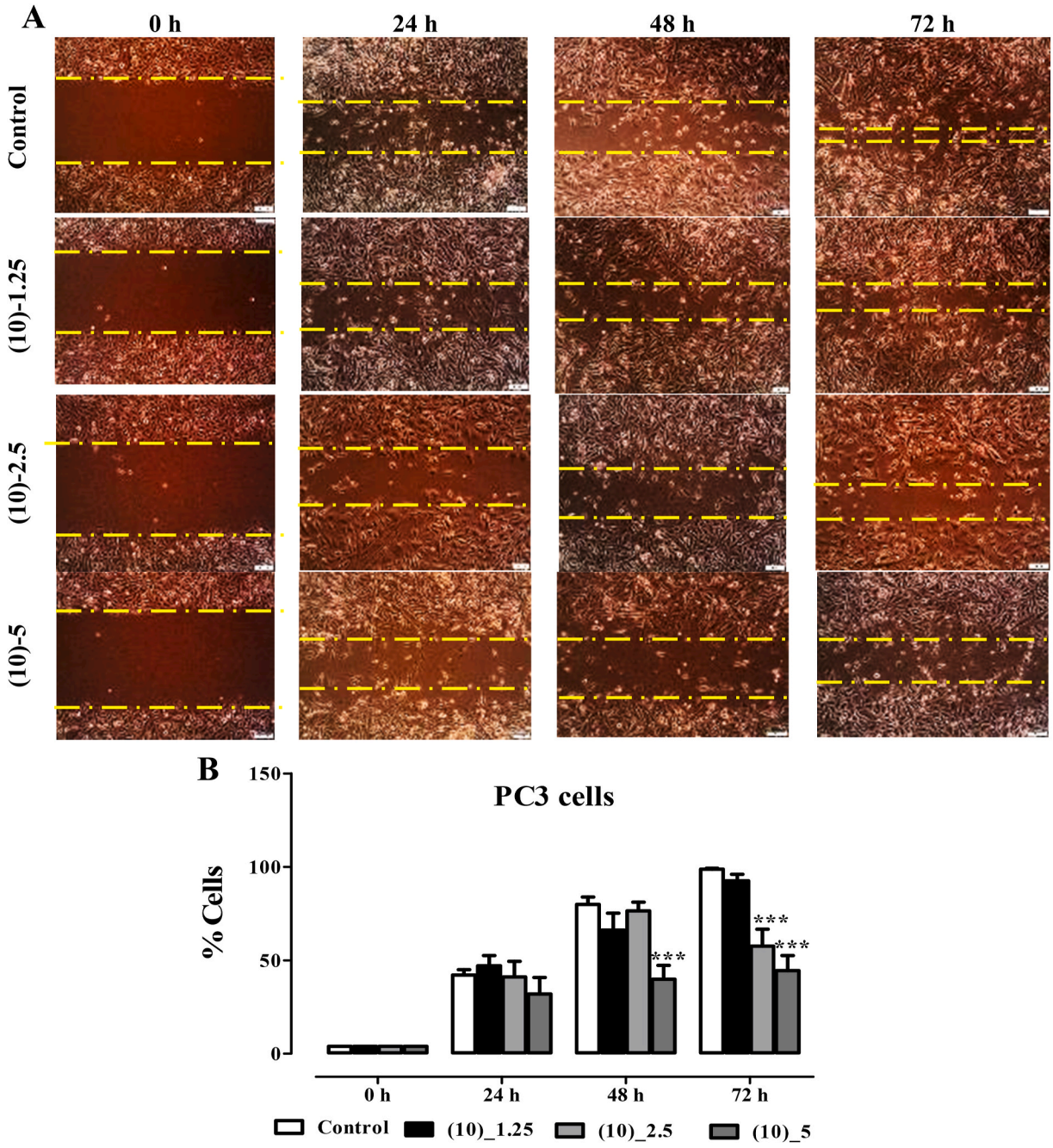

Fig. 9. Effects of compounds **10** on PC3 cells migration. Microphotographs of one assay (**A**) and graphic representation of three independent wound-healing assays (**B**) in PC3 cells migration after 72 h of treatment in serum free RPMI 1640 medium. ***$p < 0.001$ as compared with control.

significantly ($p < 0.01$) inhibited prostate cancer cell invasion and significantly increased cell adherence to extracellular matrix proteins such as fibronectin and collagen. This latter potential of compounds regarding cell adhesion is of great importance since it triggers the cell to remain at their primary site. Both compounds were able to inhibit cell migration, probably through the inhibition of the PI3K/AKT pathway, a pathway involved in cell survival and tumor metastasis, or through the modulation of Epithelial–mesenchymal transition (EMT) markers such as E-cadherin, N-cadherin, Snail, and vimentin (Roche, 2018; Rascio et al., 2021). As observed, compound **10** was able to decrease the level of expression of pAkt/Akt, N-cadherin, and VEGF proteins while it upregulated the expression of vimentin and β-catenin. VEGF is an important marker in angiogenesis and a key driver in tumor vascularization, and studies have shown that several strategies that target VEGF and its cognate receptors, VEGFR-1 and VEGFR-2, have been designed to treat cancer (Mabeta and Steenkamp, 2022). Thus, demonstrating the potential of compound **10** to be considered as a potential anticancer candidate if toxicity studies are met.

5. Conclusion

Among the tested compounds, **2** (Masticadienonic Acid) and **10** (kerstinginone) showed significant and concentration-dependent inhibition of PC3 and LNCaP cell growth with optimal concentrations ranging from 10 to 40 μg/mL for compound **2**, while compound **10** exhibited potent cell growth arrest at concentrations of 2.5–10 μg/mL. These two compounds showed inhibition of cell proliferation and clones formation. Compound **2** induced apoptosis only in the androgen-

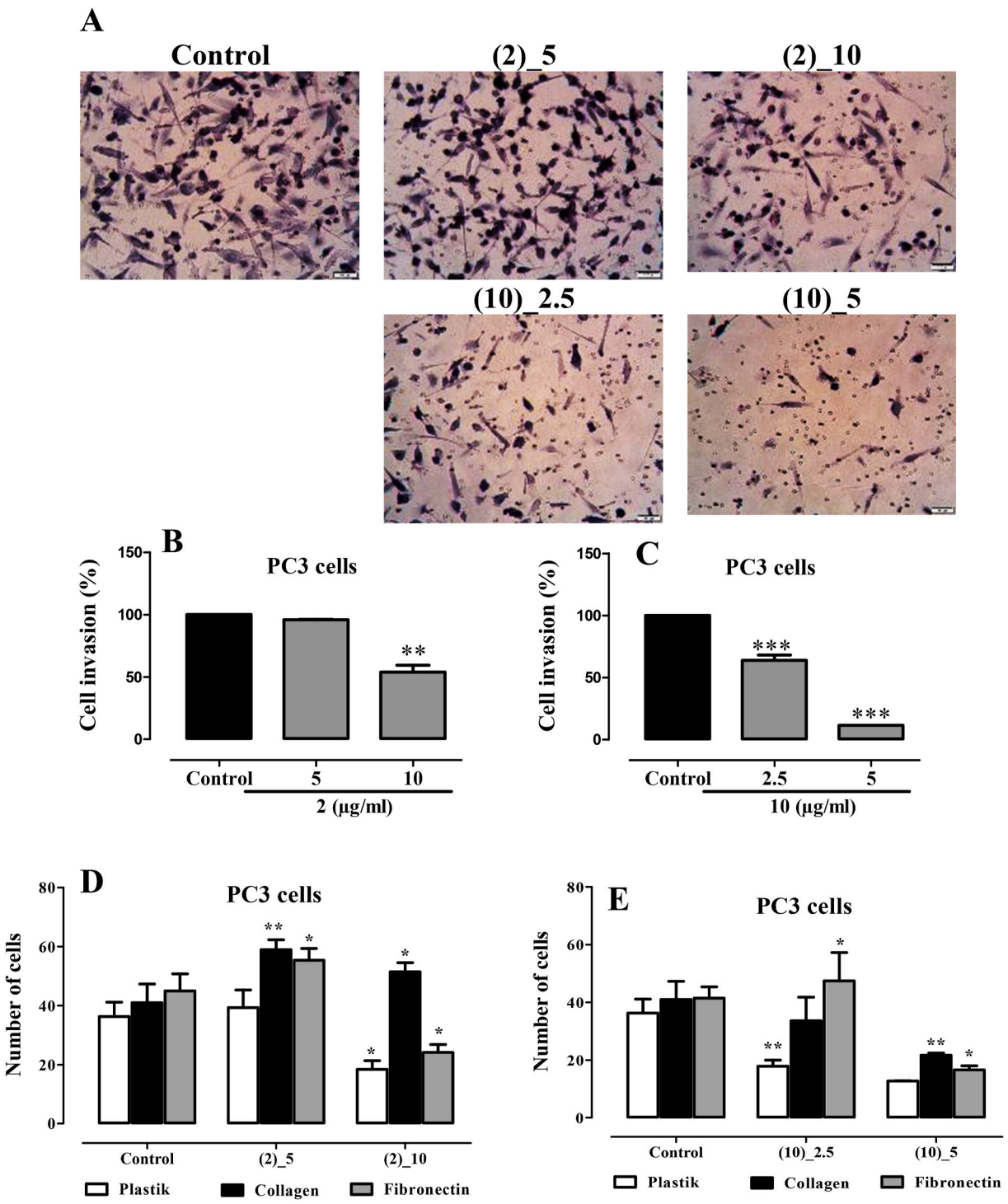

Fig. 10. Evaluation of chemotaxis of PC3 cells in the presence or absence (control) of compounds **2** (5 and 10 µg/mL) and **10** (2.5 and 5 µg/mL): microphotographs of one assay (**A**) and graphic representations of three independent assays (**B** for **2** and C for **10**). Serum-induced chemotactic movement was examined using 6-well transwell chambers with 8-µm pores. Adhesive behavior of PC3 cell lines in presence of **2** (**D**) and **10** (E). The plates were coated with extracellular matrix components (collagen or fibronectin) overnight. $^{*}p < 0.05$, $^{**}p < 0.01$ and $^{***}p < 0.001$ versus controls.

sensitive LNCaP prostate cancer cells, while compound **10** induced a stronger and concentration-dependent apoptotic effect in both PC3 and LNCaP cells with about 50–70% of apoptotic cells. It also induced potent cell migration/invasion arrest at concentrations ranging from 2.5 to 5 µg/mL and increased cell adhesion to the extracellular matrix. Kerstinginone has potent cytotoxicity and apoptosis-inducing activity, and can be a good lead for discovering a new anticancer drug.

CRediT authorship contribution statement

Joël Abel Gbaweng Yaya: Writing – original draft, Validation, Investigation, Data curation, Conceptualization. **Stephane Zingue:** Writing – original draft, Validation, Investigation, Data curation, Conceptualization. **Anne Offermann:** Writing – review & editing, Methodology, Conceptualization. **Roméo Feunaing Toko:** Methodology. **Duan Kang:** Methodology. **Elisée Bapong:** Methodology. **Céline**

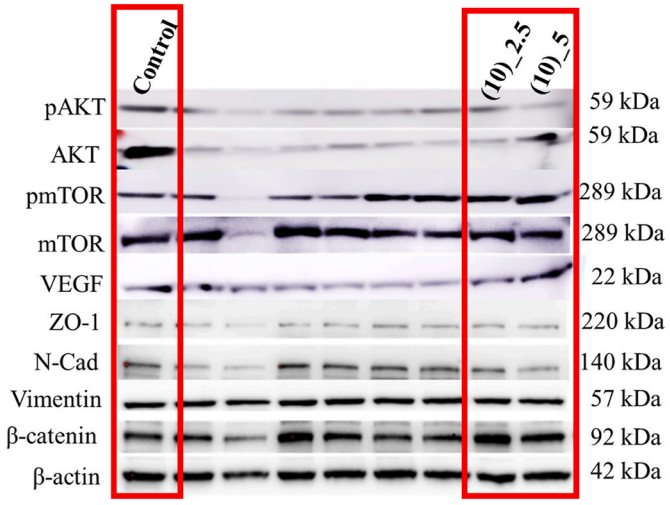

Fig. 11. Protein expression profile of some cell signaling proteins in PC3 cells treated for 48 h with compounds **2** and **10**.

Henoumont: Methodology. **Sophie Laurent:** Methodology. **Verena-Wilbeth Sailer:** Writing – review & editing, Methodology. **Jutta Kirfef:** Writing – review & editing, Methodology. **Emmanuel Talla:** Writing – review & editing, Data curation. **Sven Perner:** Writing – review & editing, Supervision, Resources, Conceptualization.

Declaration of competing interest

The authors declare no conflict of interest.

Acknowledgements

The authors are grateful to the International Foundation for Science (IFS) which supported this work through the grant number I1-F-6564-1 to Dr. YAYA G. Abel Joel. This work has been performed with the support from OPCW (Organization for the Prohibition of Chemical Weapons) to Prof. Dr. Stephane Zingue (Grant N° OPCW 188/22 1/3 INS). We thank the bioprofiling platform supported by the European Regional Development Fund and the Walloon Region, Belgium.

Appendix A. Supplementary data

Supplementary data to this article can be found online at https://doi.org/10.1016/j.jep.2024.119073.

Data availability

Data will be made available on request.

References

Bray, F., Ferlay, J., Soerjomataram, I., Siegel, R.L., Torre, L.A., Jemal, A., 2018. Global cancer statistics 2018: GLOBOCAN estimates of incidence and mortality worldwide for 36 cancers in 185 countries. CA A Cancer J. Clin. 68, 394–424.

Chi-Yu, G., Jun-Li, Z., 2018. Bioactive sesquiterpenoids and steroids from the resinous exudates of Commiphora myrra. Nat. Prod. Res. 8p. https://doi.org/10.1080/14786419.2018.1448811.

Choi, Y.J., Choi, Y.K., Lee, K.M., Cho, S.G., Kang, S.Y., Ko, S.G., 2016. Sh003 induces apoptosis of DU145 prostate cancer cells by inhibiting ERK-involved pathway. BMC Compl. Alternative Med. 16, 507.

Cojoc, M., Peitzsch, C., Kurth, I., Trautmann, F., Kunz-Schughart, L.A., Telegeev, G.D., Stakhovsky, E.A., Walker, J.R., Simin, K., Lyle, L., Fuessel, S., Erdmann, K., Wirth, M. P., Krause, M., Baumann, M., Dubrovska, A., 2015. Aldehyde dehydrogenase is regulated by β-catenin/tcf and promotes radioresistance in prostate cancer progenitor cells. Cancer Res. 75, 1482–1494.

Djoukeng, J.D., Abou-Mansour, E., Tabacchi, R., Tapondjou, A.L., Bouda, H., et al., 2005. Antibacterial triterpenes from *Syzygium guineense* (myrtaceae). J. Ethnopharmacol. 101, 283–286.

Ferlay, J., Ervik, M., Lam, F., Colombet, M., Mery, L., Piñeros, M., Znaor, A., Soerjomataram, I., Bray, F., 2020. Global cancer observatory: cancer today. Lyon, France. International Agency for Research on Cancer. https://gco.iarc.fr/today, 13 October 2022.

Hussar, P., 2022. Apoptosis Regulators Bcl-2 and Caspase-3. *Encyclopedia*, vol. 2, pp. 1624–1636.

Hutchinson, J., Dalziel, J.M., 1966. Flora of West Tropical Africa, second ed. Crown Agents for Overseas Governments and Administration. The Whitefrias Press Ltd, London, pp. 694–697. Vol I. part I.

Jaglanian, A., Deborah, T., Evangelia, T., 2020. Rosemary (*Rosmarinus officinalis* L.) extract inhibits prostate cancer cell proliferation and survival by targeting Akt and mTOR. Biomed. Pharmacother. 131, 2020.

Jia-Wang, L., Ying, L., Yong-Ming, Y., Jing, Y., Xi-Feng, L., Yong-Xian, C., 2018. Commiphoratones A and B, two sesquiterpene dimers from resina *Commiphora. Org. let.* 4pp. https://doi.org/10.1021/acs.orglett.8b00561.

Jing, X., Yuanqiang, G., Peng, Z., Ping, G., Yonggang, M., Chunfeng, X., Da-qing, J., Liping, G., 2012. Four new sesquiterpenes from *Commiphora myrra* and their neuroprotective effects. Fitoterapia 83, 801–805.

Judith, U., Svenja, S., Alexis, S.G., Menna, E.G., Thomas, S., Tatiana, S., Michael, S., 2022. Phytochemical composition of *Commiphora oleogum* resins and their cytotoxicity against skin cancer cells. Molecules 27, 3903.

Kazuyoshi, K., Marwani, E., Kobayashi, A., Nitoda, T., Kanzaki, H., 1998. Production of antibacterial triterpenes acids not detected in the native plant by cell suspension culture of Tectona grandis. Sci. Rep. Facul. Agric. 87, 9–12. Okayama University.

Keay, R.W.J., 1964. Nigerian Trees Vol II. Clavendon Press, Oxford, UK, pp. 248–257.

Liumir, O.H., Tomas, R., Valery, M.B., Arieh, M., 2005. Myrrh-*Commiphora* chemistry. Biomed. Pap. 149, 3–28.

Mabeta, P., Steenkamp, V., 2022. The VEGF/VEGFR Axis revisited: implications for cancer therapy. Int. J. Mol. Sci. 23, 15585.

Macfarlan, T.S., Gifford, W.D., Driscoll, S., Lettieri, K., Rowe, H.M., Bonanomi, D., Firth, A., Singer, O., Trono, D., Pfaff, S.L., 2012. Embryonic stem cell potency fluctuates with endogenous retrovirus activity. Nature 487, 57–63.

Mann, A., Gbate, M., Umar, A.N., 2003. Medicinal and Economic Plants of Nupeland, first ed. Jube Evans Books and Publications, Nigeria.

Maria, C.M., Ornelio, R., Daniela, L., 2018. Phytochemistry of *Commiphora erythraea*: a review. Nat. Prod. Commun. 13, 1209–1212.

Musa, A.A., 2008. Antioxidant and antibacterial activity of *Commiphora kerstingii* Engl. Stem bark extract. Res. J. Phytochem. 2, 106–111.

Ortega, M.M.A., Segura, C.M.R., 2021. Macronutrients and micronutrients in cancer prevention and treatment. Oncol Funct. Nut. 99–124.

Pernar, C.H., Ericka, M.E., Kathryn, M.W., Lorelei, A.M., 2018. The epidemiology of prostate cancer. Cold Spring Harb. Perspect. Med. 8a., 030361

Prashanth, R., 2019. Epidemiology of prostate cancer. World J. Oncol. 10, 63–89.

Promsattha, R., Tempesta, M.S., Fomum, Z.T., Ayafor, J.F., Mbafor, J.T., 1986. Sigmoidin D: a new prenylated flavanone from *Erythrina sigmoidea*. J. Nat. Prod. 49, 932–933.

Rascio, F., Spadaccino, F., Rocchetti, M.T., Castellano, G., Stallone, G., Netti, G.S., Ranieri, E., 2021. The pathogenic role of PI3K/AKT pathway in cancer onset and drug resistance: an updated review. Cancers 13, 3949.

Rawla, P., 2019. Epidemiology of prostate cancer. World J. Oncol. 10, 63–89.

Roche, J., 2018. The epithelial-to-mesenchymal transition in cancer. Cancers 10, 52.

Sallau, M.S.K., 2009. Phytochemical and Pharmacological Studies of the Leaves of *Commiphora Kerstingii* Engl (Burseraceae). Thesis, Department of Pharmaceutical and Medicinal Chemistry, Faculty of Pharmaceutical Sciences. Ahmadu Bello University, Zaria-Nigeria.

Sara, M., Khedidja, B., Mohamed, Y., 2021. Identification of 3-Methoxycaroachromene and Masticadienic acid as new traget inhibitors against trypanothione reductase from *Leisshmania infantum* using molecular docking and ADMET prediction. Molecules 26, 3335.

Shishodia, S., Chaturvedi, M.M., Aggarwal, B.B., 2007. Role of curcumin in cancer therapy. Curr. Probl. Cancer 31, 243–305.

Soufi, A., Donahue, G., Zaret, K.S., 2012. Facilitators and impediments of the pluripotency reprogramming factors' initial engagement with the genome. Cell 151, 994–1004.

Toma, I., Gidado, Khan, M., Abel, A., 2016. Phytochemical screening, antioxidant and antibacterial activities of *Commiphora* kerstingii. IBBJ 2, 8p.

Yaya, G.A.J., Hadidjatou, D., Zingue, S., Talla, E., Tchinda, T.A., Frédérich, M., Mbafor, T.J., 2018. Excelsanone, a new isoflavonoid from *Erythrina excelsa* (Fabaceae), with *in vitro* antioxidant and in vitro cytotoxic effects on prostate cancer cells lines. Nat. Prod. Res. 9. https://doi.org/10.1080/14786419.2018.1495639.

Yenesew, A., Midiwo, J.O., Miessner, M., Heydenreich, M., Peter, M.G., 1998. Two prenylated flavanones from stem bark of *Erythrina burttii. Phytochemistry*, 48, 1439–1443.

Zhang, J., Kurita, M., Shinozaki, T., Ukiya, M., Yasukawa, K., et al., 2014. Triterpene glycosides and other Polar constituents of shea (*Vitellaria paradoxa*) kernels and their bioactivities. Phytochemistry 108, 157–170.

Zingue, S., Yaya, G.A.J., Cislotto, J., Kenmogne, L.V., Talla, E., Bishayee, A., Njamen, D., Creczynski-Pasa, T.B., Ndinteh, T.D., 2020. Abyssinone V-4' methyl ether, a flavanone isolated from *Erythrina droogmansiana*, exhibits cytotoxic effects on human breast cancer cells by induction of apoptosis and suppression of invasion. Evid. base Compl. Alternative Med. 14p.